Transannular Effects in Dicobalta−Superphane Complexes on the Mixed-Valence Class II/Class III Interface: Distinguishing between Spin and Charge Delocalization by Electrochemistry, Spectroscopy, and ab Initio Calculations

Michael E. Stoll,[†] Sherri R. Lovelace,[†] William E. Geiger,*[,†] Holger Schimanke,[‡] Isabella Hyla-Kryspin,[‡] and Rolf Gleiter*[,‡]

Contribution from the Department of Chemistry, University of Vermont, Burlington, Vermont 05405, and Organisch-Chemisches Institut der Universitat Heidelberg, Im Neuenheimer Feld 270, 69120 Heidelberg, Germany

Received May 5, 1999

Abstract: The oxidative electron-transfer properties of several superphane complexes consisting of cyclopentadienylcobalt cyclobutadiene moieties linked by either three (compounds **1** and **4**) or five (compounds **2** and **5**) bridging methylene groups have been studied by experimental and theoretical methods. In both cases two separate one-electron oxidations are found. The mixed-valent monocations of the $(-CH_2-)_5$-bridged complexes are valence-trapped with very weak interactions between metal centers. The $(-CH_2-)_3$ complexes, however, have strong interactions between the two molecular halves. The intervalence transfer (IT) band of $\mathbf{1}^+$ has characteristics of both class II (localized) and class III (delocalized) behavior, but the IR spectra of carboxy-labeled $\mathbf{4}^+$ clearly establish trapped valence for the monocations of the propano-bridged systems. Photoelectron spectra and ab initio calculations at the UHF level show that, in the ground electronic state, $\mathbf{1}^+$ has a half-filled orbital (i.e., electron *spin*) that is essentially localized in one Co d_{xy}, orbital, but that the *charges* on the two metals are unequal owing to inductive electronic effects which give unequal electron flow from the ligands to the two metal centers. Calculations and IR (carbonyl) spectral shifts suggest about a 70:30 charge ratio between the two metal centers in $\mathbf{1}^+$ and $\mathbf{4}^+$, whereas both spin and charge localization is virtually complete in the pentano-bridged complexes $\mathbf{2}^+$ and $\mathbf{5}^+$. The intervalence transition in $\mathbf{1}^+$ is proposed to proceed through a "hole"-transfer process mediated by a π-cyclobutadiene MO, ultimately involving a through-bond transannular mechanism.

Introduction

There is strong continuing interest in defining the consequences of transannular π/π interactions on chemical and physical properties, including those involving donor−acceptor and electron-transfer processes.[1] Cyclophanes,[2a,b] (e.g., **A**) in general, and superphanes,[2c] (e.g., **B**) in particular, are attractive models for the investigation of such phenomena. Superphanes have the advantage of fixing the π/π interaction distance owing to their molecular rigidity at the point of transannulation. Spectroscopic studies and theoretical calculations have been helpful[3] in showing that both through-space (π/π) effects and through-bond effects (via methylene or other bridges) may influence interactions between the two linked moieties. The dicobalt complexes (**C**) are potentially useful for studies of electron transfer across the transannular face since the CpCo-(η^4-C_4R_4) group is a redox-active moiety.[4] Furthermore, some

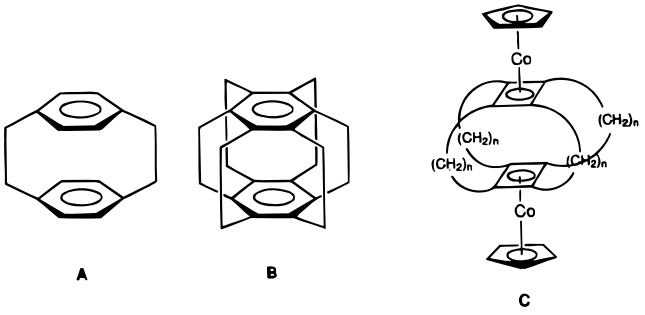

measure of control of the distance between the electron-transfer centers may be asserted by alterations in the number of bridging methylene groups in the bridges.[3] A preliminary study[5] showed that differences between the potentials of the two successive Co(I)/Co(II) oxidation waves of the dinuclear complexes increased as the number of bridging methylene groups became smaller, with the separation (Δ) of $E_{1/2}$ values going from about 450 mV in (propano-bridged) **1** to 150 mV in (pentano-bridged) **2** to 80 mV in (heptano-bridged) **3**. Observations of this type are commonly interpreted in terms of diminishing site−site interactions with smaller $\Delta E_{1/2}$ values,[6] but there are notable

[†] University of Vermont.
[‡] Universitat Heidelberg.

(1) Hall, D. B.; Barton, J. K. *J. Am. Chem. Soc*. **1997**, *119*, 5045 and references therein.

(2) (a) Keehn, P. H., Rosenfeld, S. M., Eds. *Cyclophanes*; Academic Press: New York, 1983; Vol. I. (b) Voegtle, F., Ed. Cyclophanes I and II. *Topics in Current Chemistry*; Springer-Verlag: Berlin, 1983; Vols. 113 and 115. (c) Boekelheide, V. *Accounts Chem. Research* **1980**, *13*, 65. (c) Gleiter, R.; Kratz, D. *Acc. Chem. Res*. **1993**, *26*, 311.

(3) Kovac, B.; Mohraz, M.; Heilbronner, E.; Boekelheide, V.; Hopf, H. *J. Am. Chem. Soc*. **1980**, *102*, 4314.

(4) Koelle, U. *Inorg. Chim. Acta* **1981**, *47*, 13.

(5) Gleiter, R.; Roeckel, H.; Pflaesterer, G.; Treptow, B.; Kratz, D. *Tetrahedron Lett*. **1993**, *34*, 8075.

10.1021/ja9914792 CCC: $18.00
Published on Web 09/24/1999

exceptions that reduce the generality of this correlation. For example, a series of helicene−bisquinone compounds was shown by Liberko et al. to have (cathodic) $\Delta E_{1/2}$ values from 270 to 470 mV, but all of the monoanion radicals in the series were completely delocalized (class III) systems on the ESR time scale.[7] Similarly, some metal-containing systems with small $\Delta E_{1/2}$ values have been shown to be delocalized on the time scales of IR spectroscopy (Os metals with a μ-pyrazine bridge, $\Delta E_{1/2} = 250$ mV)[8a] or Mossbauer spectroscopy (Fe metals with a μ-biphenyl bridge, $\Delta E_{1/2} = 150$ mV).[8b] Since infrared spectroscopy is usually the least ambiguous probe to charge-transfer delocalization in mixed-valent species,[9] we decided to investigate the oxidation products of the dicobalt superphane series by this method. A carbonyl group introduced into the cyclopentadienyl ligand as an ester functionality serves as the IR label, since a −COR− group undergoes a measurable shift in ν_{CO} with a change in metal oxidation state for metal−cyclopentadienyl complexes.[10]

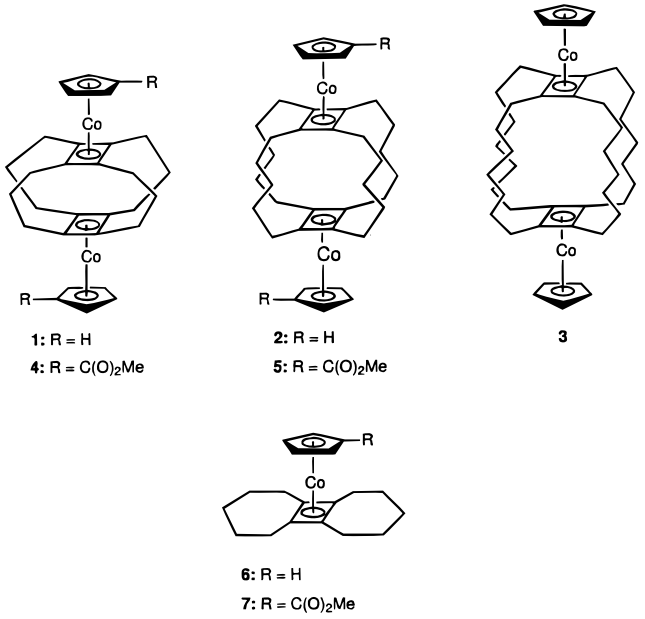

The complexes with strongly interacting metal centers, i.e., the propano-bridged systems **1** (R = H) and **4** (R = CO_2Me), are of greatest interest. As potentially intrinsically delocalized mixed-valent systems, they have relevance to the current interest in polymetallic systems on the interface of class II/class III behavior.[11−17] The transannular distance in these compounds has been determined by X-ray crystallography to be about 3.0 Å, easily within the 3.4 Å necessary for overlap of linearly-directed carbon p-orbitals. Since their relatively large $\Delta E_{1/2}$ values[5] are above the "limit" normally associated with trapped mixed-valent systems,[18] there are both intuitive and experimental reasons to expect $\mathbf{1}^+$ and $\mathbf{4}^+$ to be valence-delocalized. The present study, however, presents IR spectra suggesting that the monocation $\mathbf{4}^+$ is *valence-trapped*, just as is its elongated analogue $\mathbf{5}^+$. The optical spectra of $\mathbf{1}^+$ and $\mathbf{4}^+$ are less definitive, since the intervalence transition (IT band) shares characteristics of both trapped-valent and valence-delocalized behavior. Photoelectron spectra of the neutral compounds and ab initio (HF and UHF) calculations on both the neutral compounds and their monocations resolve these divergent observations in favor of the valence-trapped model. It is shown that the *electron spin* is essentially localized on half of the molecule in $\mathbf{1}^+$ and $\mathbf{4}^+$, but that the *electronic charge* is more highly distributed over both molecular halves.

Experimental Section

All chemical and electrochemical manipulations were conducted under nitrogen using conventional Schlenk techniques or in a Vacuum Atmospheres Co. drybox. All glassware was either flame dried or removed from a 120 °C oven and immediately placed under vacuum to cool. Solvents were dried with appropriate drying agents: CH_2Cl_2 (Omnisolv grade), CaH_2; acetone (Aldrich HPLC grade), $CaSO_4$ (then stored over molecular sieves); 1,2-difluorobenzene (Strem), alumina. Acetonitrile (Aldrich spectrophotometric grade) was placed over 3 Å molecular sieves and stored in the drybox. Deoxygenation of the solvents was performed by sparging with nitrogen gas for chemical oxidations and by three successive freeze−pump−thaw cycles on a high-vacuum line for electrochemical experiments. The solvents for electrochemistry were vacuum-transferred just prior to use.

Chemicals. The cobalt complexes were prepared as described earlier,[19] as was acetylferrocenium tetrafluoroborate.[20] The supporting electrolyte $[Bu_4N][PF_6]$ was recrystallized from ethanol and vacuum-dried at 373 K.

Electrochemistry. Traditional three-electrode, three-compartment cell geometry was employed for both voltammetry and bulk electrolyses, usually with a Ag/AgCl reference electrode separated from the test solution by a fine frit. An internal standard of ferrocene or decamethylferrocene was added near the end of each experiment to calibrate the potentials, and all potentials in this paper are reported versus the ferrocene/ferrocenium couple in CH_2Cl_2. Conversions from the decamethylferrocene scale to the ferrocene scale was done by addition of 0.55 V.[21] The $E_{1/2}$ values reported for chemically reversible systems are the average of the observed anodic and cathodic peak potentials. A supporting electrolyte concentration of 0.1 M was employed unless otherwise noted. The working electrode for cyclic voltammetry was a Pt disk of either 0.5 or 2 mm diameter. It was polished with successively finer alumina slurries down to l μm. For bulk electrolysis a cylindrical Pt gauze electrode was used.

A PARC model 173 potentiostat was interfaced to an IBM-compatible PC through a PARC model 276 interface. The PC served as a waveform generator and digital recorder through the use of a DOS-

(6) (a) Ward, M. D. *Chem. Soc. Rev.* **1995**, *121*. (b) Richardson, D. E.; Taube, H. *Coord. Chem. Rev.* **1984**, *60*, 107. (c) Crutchley, R. J. *Adv. Inorg. Chem.* **1994**, *41*, 273. (d) Newton, M. D. Chem. Rev. **1991**, *91*, 767.

(7) Liberko, C. A.; Miller, L. L.; Katz, T. J.; Liu, L. *J. Am. Chem. Soc.* **1993**, *115*, 2478.

(8) (a) Gloeckle, M.; Kaim, W.; Fiedler, J. *Organometallics* **1998**, *17*, 4923. (Os_2 with a μ-pyrazine bridge, $\Delta E_{1/2} = 250$ mV, but delocalized by IR). (b) Lacoste, M.; Rabaa, H.; Astruc, D.; Ardoin, N.; Varret, F.; Saillard, J.-Y.; LeBeuze, A. *J. Am. Chem. Soc.* **1990**, *112*, 9548 (Fe_2 with a μ-biphenyl bridge, $\Delta E_{1/2} = 130$ mV, but delocalized by Mossbauer).

(9) Chin, T. T.; Grimes, R. N.; Geiger, W. E. *Inorg. Chem.* **1999**, *38*, 93 and references therein.

(10) Atwood, C. G.; Geiger, W. E.; Bitterwolf, T. E. *J. Electroanal. Chem.* **1995**, *397*, 279. ν_{CO} increases by 35 cm^{-1} when acetylferrocene is oxidized to the corresponding ferrocenium ion.

(11) McManis, G. E.; Nielson, R. M.; Weaver, M. J. *Inorg. Chem.* **1988**, *27*, 1827.

(12) Demadis, K. D.; El-Samonody, E. S.; Coia, G. M.; Meyer, T. J. *J. Am. Chem. Soc.* **1999**, *121*, 535.

(13) Atwood, C. G.; Geiger, W. E.; Rheingold, A. L. *J. Am. Chem. Soc.* **1993**, *115*, 5310.

(14) Manriquez, J. M.; Ward, M. D.; Reiff, W. M.; Calabrese, J. C.; Jones, N. L.; Carroll, P. J.; Bunel, E. E.; Miller, J. S. *J. Am. Chem. Soc.* **1995**, *117*, 6182.

(15) Evans, C. E. B.; Naklicki, M. L.; Rezvani, A. R.; White, C. A.; Kondratiev, V. V.; Crutchley, R. J. *J. Am. Chem. Soc.* **1998**, *120*, 13096.

(16) Rocha, R. C.; Araki, K.; Toma, H. E. *Inorg. Chim. Acta.* **1999**, *285*, 197.

(17) Jones, P. L.; Jeffery, J. C.; Maher, J. P.; McCleverty, J. A.; Rieger, P. H.; Ward, M. D. *Inorg. Chem.* **1997**, *36*, 3088.

(18) (a) Lee, M.-T.; Foxman, B. M.; Rosenblum, M. *Organometallics* **1985**, *4*, 539. (b) Gilbert, A. M.; Katz, T. J.; Geiger, W. E.; Robben, M.; Rheingold, A. L. *J. Am. Chem. Soc.* **1993**, *115*, 3199.

(19) Gleiter, R.; Pflaesterer, G. *Organometallics* **1993**, *12*, 1886.

(20) Connelly, N. G.; Geiger, W. E. *Chem. Rev.* **1996**, *96*, 877.

(21) We measure $E_{1/2}$(ferrocene) − $E_{1/2}$(decamethylferrocene) = 0.55 V in CH_2Cl_2/0.1 M [NBu4][PF_6].

based program developed in-house by Dr. Michael J. Shaw. For IR spectroelectrochemical experiments employing a thin-layer cell, the potentiostat was equipped with a PARC model 179 digital coulometer and used independently of a waveform generator. For spectroelectrochemical experiments employing a fiber-optic "dip" probe, the PARC Model 173 potentiostat was used in conjunction with a PARC model 175 waveform generator for voltammetry and a PARC model 179 digital coulometer for bulk electrolysis. Voltammetry data were recorded on a Yokogawa model 3023 *X*−*Y* recorder when the fiber-optic probe was employed.

IR Spectroelectrochemistry. Infrared spectroelectrochemistry was performed either with an IR transparent thin layer electrode (IRTTLE) cell[10] housed in the sample compartment of a Mattson Polaris FTIR spectrometer operating at 2 cm^{-1} resolution or with a fiber-optic dip probe (Remspec, Inc.) which was sent through the drybox wall into an electrolysis cell. The volume of the IRTTLE cell (typically 75 μL) was calibrated by coulometry on a known concentration of acetylferrocene.

Operation of the fiber-optic dip probe under Schlenk conditions has been previously described.[22] A drybox was modified so that the probe can be used directly inside of the box with a typical three-compartment electrolysis cell. The probe is simply passed through a hole in the side of the box and sealed on the inside with a piece of large-diameter Tygon tubing that fits snugly on the top of the probe. This method offers the advantage of more rigorous exclusion of oxygen and moisture during the experiment compared to the Schlenk techniques that were previously employed.[22] The voltammetry of the analyte solution can then be accurately monitored during the experiment to support the IR results. Accurate temperature control was obtained with a cooling bath consisting of 2,2,4-trimethylpentane as the cooling solution and an FTS Systems model FC100A01 cooling probe.

In a typical IRTTLE cell experiment a stock solution of supporting electrolyte (0.4−0.5 M) and solvent was introduced into the cell. A spectrum of this solution was recorded and used as the active background for subsequent scans. The analyte was then dissolved in an appropriate volume of the stock supporting electrolyte solution to give an analyte concentration of 2−3 mM. The analyte solution was introduced into the cell, a spectrum of the initial solution was obtained, and the electrolysis was started. Spectra were then recorded at times during the electrolysis that were correlated with the coulometry of the conversion. The electrolysis was stopped during IR acquisition, which usually consisted of 32 replicate scans requiring about 1.2 min of total acquisition time.

The fiber-optic probe was used in conjunction with bulk electrolysis methods. During electrolysis and when voltammetric data were acquired, the probe was positioned above the solution in the working compartment of the cell. When an IR spectrum was needed, the electrolysis was stopped and the fiber-optic probe was inserted into the solution. The nominal concentration of analyte, 1 mM, was large enough to produce good quality spectra, but small enough to give convenient electrolysis currents. Analyte spectra were solvent/supporting electrolyte subtracted. A single spectrum consisted of an average of between 64 and 128 scans with an acquisition time of 2−4 min. The larger number of scans for the fiber-optic probe compared to the IRTTLE cell arises from the reduced S/N inherent to the probe.

Near-IR Spectra. Near-infrared/visible spectra (600-2200 nm) of the monocations were recorded on an OLIS-modified CARY 14 spectrophotometer. All spectra were recorded in a 1 cm path length screw-top quartz cuvette at ambient temperature; a spectrum of the solvent or solvent and supporting electrolyte solution was digitally subtracted from the sample spectrum. Samples obtained from bulk electrolysis experiments were syringed out of the electrochemical cell into the cuvette once the appropriate species was formed.

Near-IR spectra were also recorded for chemically-oxidized solutions of the monocations. The oxidizing agent for the chemical oxidations was acetylferrocenium tetrafluoroborate, $E^\circ = +0.270$ V vs Fc/Fc^+.[20] In a typical experiment ca. 6 mg of the neutral cobalt compound was dissolved in 2 mL of solvent. In a second vial an equimolar amount of the oxidizing agent was dissolved in another 2 mL of solvent and then added to the solution of the neutral complex. A color change immediately occurred, and the resulting solution was transferred to the cuvette, which was subsequently sealed with a screw top, removed from the drybox, and placed in the sample compartment of the instrument.

Table 1. Electrochemical Data for Oxidation of Selected Mono- and Dinuclear Cobalt Superphane Complexes in Dichloromethane[a]

compd	$E_{1/2}$(l) (V)	$E_{1/2}$(2) (V)	$\Delta E_{1/2}$(V)
6	0.06		
7	0.24		
1	−0.07	0.32[d]	0.39
4[b]	0.20	0.64[d]	0.44
2	0.05_5	0.20	0.14_5
$CpCo(C_4Ph_4)$[c]	0.45		
$CpCo[C_4(CH_3)_4]$[c]	0.05		

[a] All potentials are referenced to the ferrocene/ferrocenium couple. [b] From ref 5. [c] From ref 4. [d] Irreversible process, E_p given.

Photoelectron Spectroscopy. The He(I) photoelectron spectrum of **1** was recorded on a PS-18 photoelectron spectrometer (Perkin-Elmer) at 190 °C. The spectrum was calibrated with Ar (15.76 and 15.94 eV) and Xe (12.13 and 13.44 eV). A resolution of 20 meV on the Ar-line $^2P_{3/2}$ was obtained.

Calculational Details. Ab initio calculations on the ground-state electronic structure of **1**, **2**, $\mathbf{1}^+$, and $\mathbf{2}^+$ have been carried out at the Hartree−Fock (HF) level.[23] The doublet-state wave functions were optimized with the unrestricted (UHF) procedure. The calculations have been carried out in C_s (**1**, $\mathbf{1}^+$) and C_i (**2**, $\mathbf{2}^+$) symmetry point groups with geometrical parameters taken from X-ray data of the neutral molecules.[24] A single basis set was applied in our studies. The all-electron basis sets of respective sizes (10s,5p) and (4s) were used for carbon and hydrogen and contracted to split valence.[25] The 1s, 2s, and 2p electrons of the cobalt atoms were replaced by pseudopotentials. For the remaining electrons we have applied the (8s,5p,5d) basis set of Hay and Wadt.[26] The contraction scheme corresponds to a single-ζ description for the outermost core electrons and to a double-ζ description for the valence region. The charge distributions have been analyzed with the natural atomic orbital (NAO) method.[27] The calculations have been carried out with the Gaussian 94 program.[28]

Results

Mononuclear Complexes. Characteristics of the Redox Sites. The electrochemical and spectroscopic properties of the mononuclear systems **6** and **7** are relevant as models for the redox sites in the dinuclear complexes. Their one-electron diffusion-controlled oxidations were uncomplicated in CH_2Cl_2 at ambient temperatures, giving the corresponding 17-electron monocations $\mathbf{6}^+$ and $\mathbf{7}^+$ in chemically reversible, quasi-Nernstian processes at potentials slightly positive of the ferrocene$^{0/+}$ couple (Table 1).

When the infrared-labeled derivative **7** was exhaustively electrolyzed (Figure 1), a fiber-optic IR probe revealed a shift

(22) Shaw, M. J.; Geiger, W. E. *Organometallics* **1996**, *15*, 13.

(23) Hehre, W. J.; Radom, L.; Schleyer, P. v. R.; Pople, J. A. *Ab Initio Molecular Orbital Theory*; John Wiley and Sons: New York, 1986.

(24) (a) Gleiter, R.; Karcher, M.; Ziegler, M. L.; Nuber, B. *Tetrahedron Lett.* **1987**, *28*, 195. (b) Gleiter, R.; Treptow, B.; Kratz, D.; Nuber, B. *Tetrahedron Lett.* **1992**, *33*, 1736.

(25) Dunning, T. H.; Hay, J. P. *Modem Theoretical Chemistry*; Plenum: New York, 1976; Chapter 1.

(26) Hay, J. P.; Wadt, W. R. *J. Chem. Phys.* **1985**, *82*, 299.

(27) (a) Foster, J. P.; Weinhold, F. *J. Am. Chem. Soc.* **1980**, *102*, 7211. (b) Reed, A. E.; Weinhold, F. *J. Chem. Phys.* **1983**, *78*, 4066. (c) Reed, A. E.; Curtiss, L. A.; Weinhold, F. *Chem. Rev.* **1988**, *88*. 899.

(28) Frisch, M. J.; Trucks, G. W.; Schlegel, H. B.; Gill, P. M. W.; Johnson, B. G.; Robb, M. A.; Cheeseman, J. R.; Keith, T.; Peterson, G. A.; Montgomery, J. A.; Raghavachari, K.; Al-Laham, M. A.; Zakrzewski, V. G.; Ortiz, J. V.; Foresman, J. B. Coislowski, J.; Stefanov, B. B.; Nanayakkara, A.; Challacombe, M.; Peng, C. Y.; Ayala, P. Y.; Chen, W.; Wong, M. W.; Andres, J. L.; Replogle, E. S.; Gomperts, T.; Martin, R. L.; Fox, D. J.; Binkley, J. S.; Defrees, D. J.; Baker, J.; Stewart, J. P.; Head-Gordon, M.; Gonzalez, C.; Pople, J. A. *Gaussian 94*, Revision E.2; Gaussian, Inc.: Pittsburgh, PA, 1995.

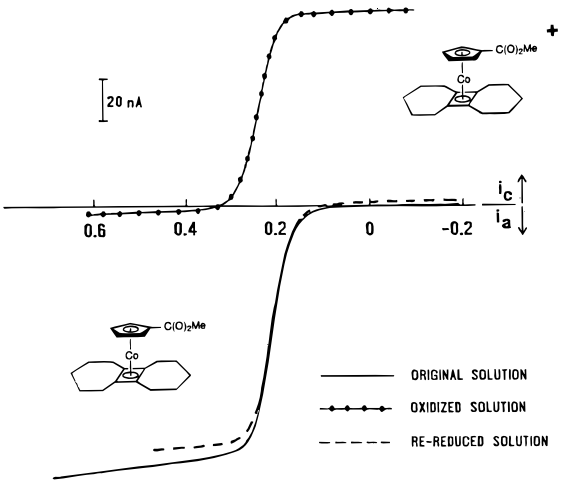

Figure 1. "Steady-state" voltammogram traces of 0.93 mM **7** (solid line, original solution; dashed line, re-reduced solution) and $\mathbf{7}^+$ (dotted line) in CH_2Cl_2/0.1 M $[NBu_4][PF_6]$ on a 500 μm Pt disk, scan rate 5 mV s^{-1}. Potentials vs ferrocene/ferrocenium couple.

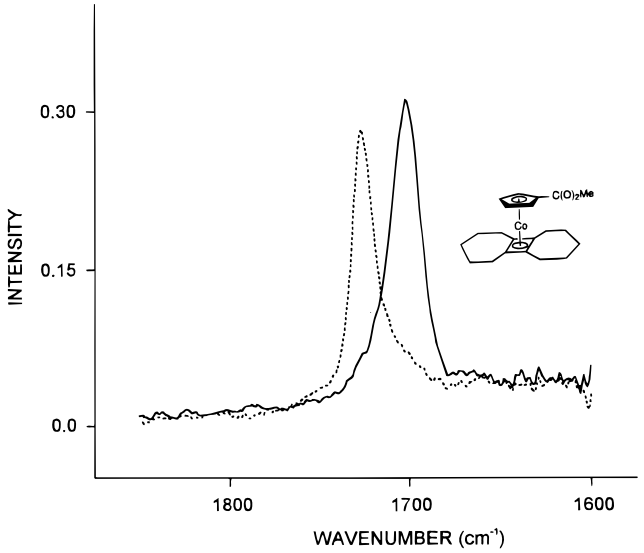

Figure 2. IR spectra in the organic carbonyl region of a 1 mM solution of **7** before (solid line) and after (dashed line) one-electron anodic electrolysis (E_{appl} = 0.50 V) in CH_2Cl_2/0.1 M $[NBu_4][PF_6]$ at 263 K using a fiber-optic probe.

Table 2. C−O Stretching Frequencies for Selected Complexes[a]

compd	ν_{CO}(neutral)	ν_{CO}(monocation) ($\Delta\nu_{CO}$)	ν_{CO}(dication) ($\Delta\nu_{CO}$)
7	1701	1726 (25)	
4	1695	1701, 1716 (6, 21)[b]	
5	1696	1696, 1721 (0, 25)	1722 (26)

[a] All frequencies are in cm^{-1}. [b] The chemical irreversibility of the second oxidation process led to decomposition of the dication $\mathbf{4}^{2+}$, thereby rendering the ν_{CO} stretching frequency for this species unobtainable.

of the carbonyl ester stretch from 1701 cm^{-1} in **7** to 1726 cm^{-1} in $\mathbf{7}^+$ (Figure 2). Combining electrolytic, voltammetric, and spectroscopic methods on the same solution raises the certitude that the spectral changes arise from the primary oxidation product $\mathbf{7}^+$. The shift of 25 cm^{-1} (Table 2) on formation of the Co(II) derivative is similar to the shift for the carbonyl stretch upon one-electron oxidation of acetylferrocene.[10] A near-IR spectrum of the Co(II) species was also obtained. In this case a concentrated (7.8 mM) solution of compound **6** was treated with 1 equiv of the acetylferrocenium ion, which has a formal

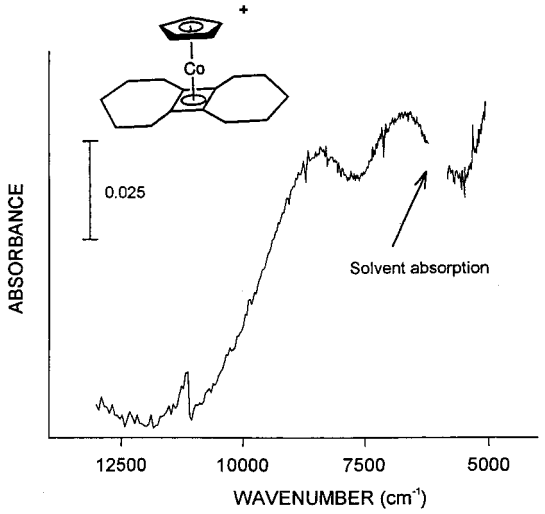

Figure 3. Near-IR spectrum of $\mathbf{6}^+$ in CH_2Cl_2 at 298 K formed by reaction of 7.8 mM **6** with 1 equiv of acetylferrocenium ion.

Table 3. Optical Transitions in the 20000−5000 cm^{-1} Range for Oxidized Species in CH_2Cl_2 Listed as Energy (Extinction Coefficient)

$\mathbf{1}^+$	12 000 cm^{-1} (600); 6100 cm^{-1} (60)[a]
$\mathbf{2}^+$	17 500 cm^{-1} (250)
$\mathbf{6}^+$	18 100 cm^{-1} (190); 8350 cm^{-1} (10); 6650 cm^{-1} (10)

[a] $\mathbf{1}^+$ in other media: difluorobenzene; 11 880 cm^{-1}; 50:50 CH_3CN/difluorobenzene, 12 200 cm^{-1}; 92:8 CH_3CN/CH_2Cl_2, 12 510 cm^{-1}; CH_2Cl_2/0.1 M $[NBu_4][PF_6]$, 12 150 cm^{-1}.

potential (0.27 V vs Fc) sufficient to oxidize **6** to $\mathbf{6}^+$. Two weak features were observed (Figure 3) at ν_{max} = 8350 and 6650 cm^{-1} which were not present in **6**, acetylferrocene, or acetylferrocenium. The very low absorbancy coefficients (ϵ ca. 10 M^{-1} cm^{-1} assuming a quantitative reaction) suggest forbidden metal d−d transitions as the origin of these features, similar to those reported for other high-symmetry 17-electron metal−cyclopentadienyl complexes.[29] The lowest energy band in the visible region for $\mathbf{6}^+$ is found at 18 100 cm^{-1} (ϵ ca. 190 M^{-1} cm^{-1}) (Supporting Information, Figure 1); optical data are collected in Table 3.

The molecular orbital description of **6** is discussed below in the section on the orbital makeup of the dinuclear complexes.

Dinuclear Complexes. Electrochemistry and Spectroelectrochemistry. I. Pentano-Bridged Complexes. The pentano-bridged complexes **2** and **5** oxidize in two reversible one-electron steps to, successively, the formal Co(II)/Co(I) and Co(II)/Co(II) complexes, e.g., $\mathbf{2}^+$ and $\mathbf{2}^{2+}$. Bulk electrolyses confirmed the one-electron nature and chemical reversibility of the oxidations. Because of the close separation of the $E_{1/2}$ values (Figure 4, $\Delta E_{1/2}$ = 145 mV), the coulometry was carefully monitored during bulk electrolyses and spectra were obtained after passage of 1 (precisely, 0.98) and then 2 (2.1) equiv of charge. The IRTTLE cell results are shown in Figure 5, wherein the ν_{CO} absorption for neutral **5** (1696 cm^{-1}) is replaced first by two bands (1696 and 1721 cm^{-1}) for $\mathbf{5}^+$ and next by a single band at higher energy, 1722 cm^{-1}, for $\mathbf{5}^{2+}$. This result is as expected for two localized charge-transfer centers, with no evidence of site−site interactions apparent from shifts in the IR energies.

The optical spectra of $\mathbf{2}^+$ were recorded on chemically (acetylferrocenium) or electrochemically oxidized solutions of **2**. A transition at 17 500 cm^{-1} (ϵ ca. 250 M^{-1} cm^{-1}) confirmed

(29) Atwood, C. G.; Geiger, W. E. *J. Am. Chem. Soc.* **1994**, *116*, 10849.

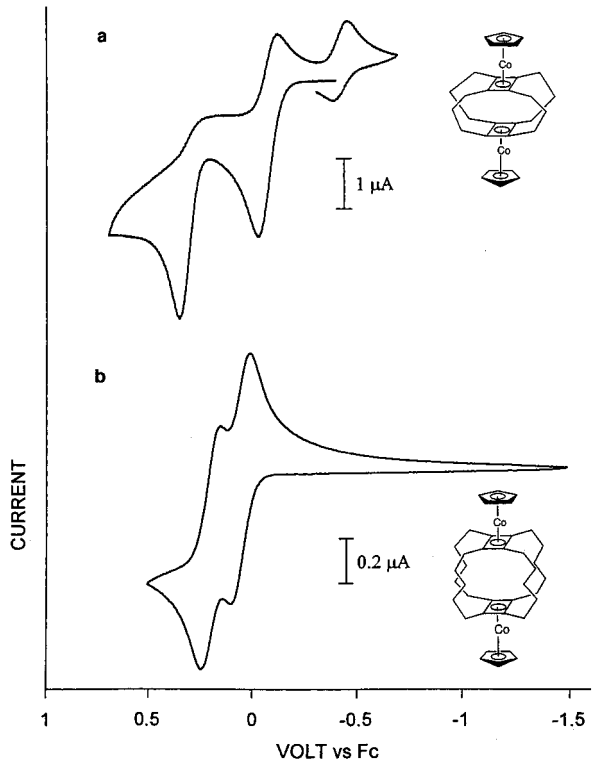

Figure 4. Cyclic voltammetry scans of **l** (top) and **2** (bottom) in CH_2Cl_2 at 298 K under the conditions (top) 0.68 mM **1**, scan rate 0.1 V s^{-1}, 2 mm Pt disk and (bottom) 1.85 mM **2**, scan rate 0.2 V s^{-1}, 500 μm Pt disk.

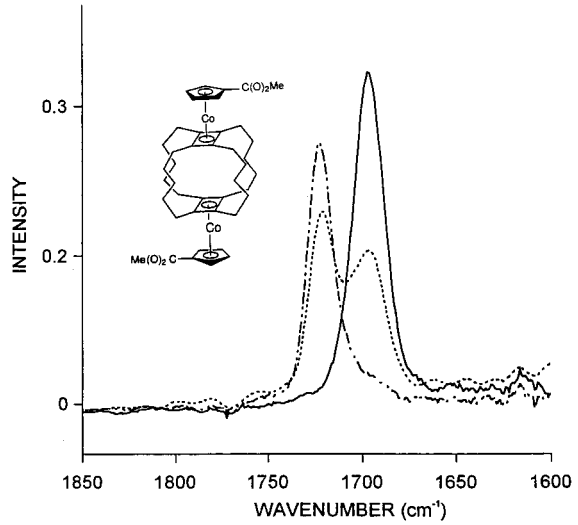

Figure 5. IR spectra in the organic carbonyl region of 4.4 mM **2** (solid line), $\mathbf{2}^+$ (dotted line), and $\mathbf{2}^{2+}$ (dotted−dashed line) in CH_2Cl_2/0.4 M $[NBu_4][PF_6]$ at 263 K using an IRTTLE cell through stepwise anodic oxidations at $E_{appl} = 0.10$ and 0.50 V.

the presence of a Co(II) site (cf. $\mathbf{6}^+$ above, band at 18 100 cm^{-1}). Attempts were made to observe an IT band for $\mathbf{2}^+$, but no extra optical bands with $\epsilon > 6$ M^{-1} cm^{-1} were observed down to energies as low as 5000 cm^{-1}. Any interactions between the metal centers in $\mathbf{2}^+$ must be quite weak.

II. Propano-Bridged Complexes. A. Infrared Spectroelectrochemistry. The propano-bridged complexes **1** and **4** undergo one-electron oxidation to monocations that are stable at room temperature in cyclic voltammetry and bulk electrolysis experiments. The second oxidations of these complexes are not reversible, however, and scanning through the second oxidation wave reveals a reversible product wave (Figure 4, top) that

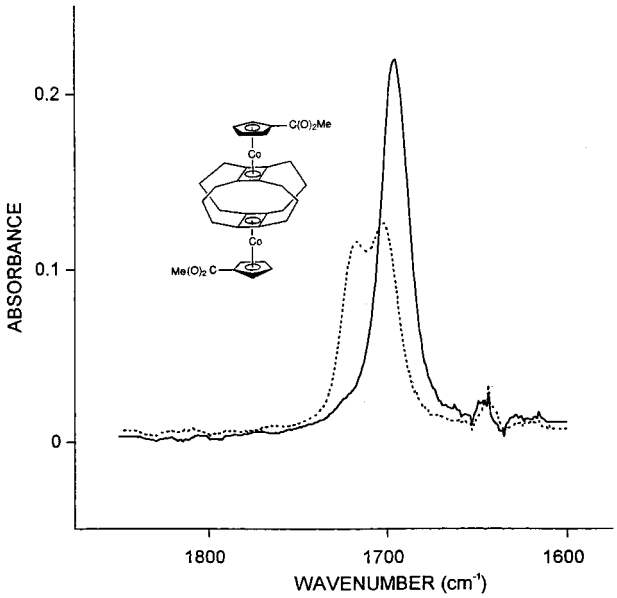

Figure 6. IR spectra in the organic carbonyl region of 2.17 mM **4** (solid line) and $\mathbf{4}^+$ (dashed line) in CH_2Cl_2/0.4 M $[NBu_4][PF_6]$ at 263 K using an IRTTLE cell with $E_{appl} = 0.45$ V.

results from the decomposition of the dication ($\mathbf{1}^{2+}$ in this case). Although this followup reaction precluded spectral characterization of the Co(II)/Co(II) dication, the mixed valence studies on the monocation were not affected.

Figure 6 shows IR spectra in the carbonyl region of ca. 2 mM **4** before electrolysis (solid line) and after passage of one charge equivalent (dotted line) in an IRTTLE cell experiment at 263 K. The single ν_{CO} band of **4** is replaced by *two* absorptions at $\nu_{CO} = 1701$ and 1716 cm^{-1} (Table 3). Although this is consistent with a *trapped-valent* description of $\mathbf{4}^+$, one notes that the two bands appear at energy shifts of 6 and 21 cm^{-1} with respect to ν_{CO} for the Co(I)/Co(I) starting material, rather than the 0 and 25 cm^{-1} shifts found upon oxidation of the pentano-bridged complex **5** (see above). Since carbonyl shifts are expected to track the metal charges, the observed shifts show that the charge separation in $\mathbf{4}^+$ is not as extreme as in $\mathbf{5}^+$ despite the fact that the monocation displays trapped valence in both cases.

B. Optical Spectroscopy. Optical spectra of $\mathbf{1}^+$ were obtained after either electrochemical or chemical oxidation of ca. 2 mM solutions of **1** in CH_2Cl_2. The band at ca. 18 000 cm^{-1} found for "localized" $CpCo^{II}Cb$ moieties is absent. Instead, two bands are found at lower energies (Figure 7), the one on the visible/near-IR border at $\nu = 12\,000$ cm^{-1} (ϵ ca. 600 M^{-1} cm^{-1}) being assigned to an IT transition, and the less intense absorption (ϵ ca. 60 M^{-1} cm^{-1}) in the near-IR region at $\nu = 6100$ cm^{-1} in CH_2Cl_2 being assigned to a ligand-to-metal charge-transfer (LMCT) transition. The origin of the latter will be better appreciated after our discussion below of the molecular orbitals of $\mathbf{1}^+$.

A combination of factors involving the solubility of **1** and the chemical stability of $\mathbf{1}^+$ limited the conditions under which the IT absorption could be investigated, but several solvents or solvent mixtures were found which allowed the energy of the band to be recorded with variations in the dielectric of the medium. The results are collected in Table 3.

Class II mixed-valent systems commonly display a linear dependence of the IT band energy on the solvent dielectric parameter $(1/D_{op} - 1/D_s)$, where D_{op} is the optical dielectric constant of the solvent and D_s is its static dielectric constant.[30]

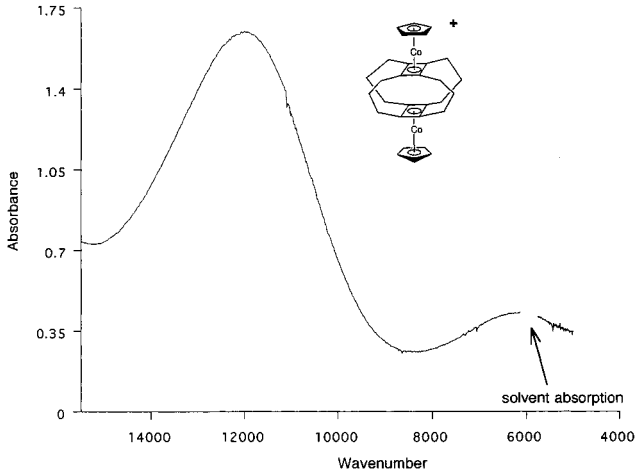

Figure 7. Visible and near-IR spectral region for $\mathbf{1}^+$ in CH_2Cl_2 generated by the reaction of 2 mM **1** with 1 equiv of acetylferrocenium ion.

Although modest agreement with this model is found (Figure 2, Supporting Information), the slope of this plot is lower than found in most class II systems.[31,32] A second diagnostic concerns the width of the IT band, $\Delta\nu_{1/2}$, compared to the Hush prediction for class II systems, $\Delta\nu_{1/2} = [2310\nu_{max}]^{1/2}$ cm^{-1}.[33] The experimental bandwidth (3.51×10^3 cm^{-1}) is considerably narrower than predicted (5.17×10^3 cm^{-1}). The usual IT criteria are less consistent, therefore, with the trapped-valent model favored by the IR data than with the delocalized (class III) behavior for $\mathbf{1}^+$. As will be shown below, the spectroscopic data are explained by a model in which the singly occupied orbital is indeed localized on half of the molecule, but that large inductive effects lead to significant overall charge (as opposed to spin) delocalization between molecular halves.

Dinuclear Complexes. Orbital Descriptions. I. Electronic Structures of Neutral 1 and 2. Photoelectron (PE) spectra are inherently informative about the electronic structures of transition-metal compounds and their singly-charged cations. It is well documented that the Koopmans theorem[34] is not valid in the case of transition-metal compounds.[35] Quantum mechanical calculations usually show that, upon ionization of metal 3d electrons, the electron density flows from the surrounding ligands toward the metal to compensate for the loss of electron density at the metal. This reorganization of electron density leads to remarkable relaxation energies and strongly diminishes the Koopmans value.[36] Correlation effects (which are too complex to be included in the present study) generally go in the opposite direction. However, it is well known that for metal ionizations the influence of relaxation remains dominant.[35,37] For ionization originating in orbitals with predominant ligand character, the global influence of relaxation and correlation is less important and never exceeds 1−2 eV.[35,37,38]

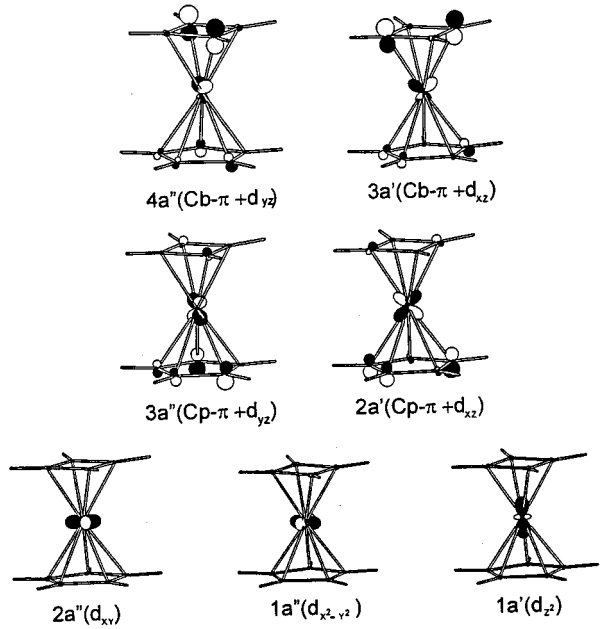

Figure 8. Highest occupied molecular orbitals of **8**, where Cp = cyclopentadienyl and Cb = cyclobutadiene.

Table 4. Koopmans Ionization Energies (eV) of **1**, **2**, and **8**

Mo type	**1**		**2**		**8**	
	symm	$-\epsilon_i$	symm	$-\epsilon_i$	symm	$-\epsilon_i$
Cb π	7a″	6.56	$7a_g$	7.18	4a″	8.0
	6a″	6.69	$6a_g$	7.22	3a′	8.0
	7a′	7.68	$7a_u$	7.29		
	6a′	7.78	$6a_u$	7.31		
Cp π	5a″	9.63	$5a_u$	10.48	3a″	9.96
	5a′	9.70	$4a_u$	10.49	2a′	9.96
	4a″	9.74	$5a_g$	10.50		
	4a′	9.80	$4a_g$	10.50		
Co t_{2g}	3a″	12.69	$3a_g$	13.46	2a″	14.0
	3a′	12.76	$3a_u$	13.53	1a″	15.29
	2a′	13.06	$2a_g$	14.01	1a′	16.43
	2a″	13.47	$2a_u$	14.11		
	1a″	14.91	$1a_g$	15.03		
	1a′	15.40	$1a_u$	15.21		

To understand the electronic structure of the ground states of **1** and **2**, we first consider the main features of the electronic structure of the mononuclear species (η^4-C_4H_4)Co(η^5-C_5H_5) (**8**), investigated earlier by PE spectroscopy,[39] which serves as a model for the individual redox sites in **1** and **2**.

The highest occupied MOs of **8** are displayed in Figure 8, and the calculated Koopmans ionization energies are presented in Table 4. The HOMO 4a″ as well as the following MOs (3a′, 3a″, and 2a′) of **8** have predominant ligand π-character with admixture of cobalt $3d_{xz}$ and $3d_{yz}$ orbitals in a bonding fashion.

There is a 2 eV energy separation between the Cp π (2a′, 3a″) and Cb π (3a′, 4a″) levels. At higher energy (16.5−14.0 eV) there are three MOs (la′, 1a″, 2a″) with predominant metal character, and consequently the cobalt atom must be formally considered as a d^6 species. Some σ MOs of the ligands are located between the ligand π and Co t_{2g} levels. These as well as the totally symmetrical π MOs centered at the ligands are omitted in Figure 8. These latter MOs do not influence the chemical behavior of **8**.

(30) Chen, P.; Meyer, T. J. *Chem. Rev.* **1998**, *98*, 1439.
(31) A slope of 2000 cm^{-1} ($R = 0.975$) is obtained for a plot of ν_{max} vs $1/D_{op} - 1/D_s$ for four different solvent systems (see the figure in the Supporting Information). Compare slopes for class II systems in, e.g., ref 32.
(32) Liu, T.-S.; Chen, Y. J.; Tai, C.-C.; Kwan, K. S. *Inorg. Chem.* **1999**, *38*, 674.
(33) See: Creutz, C. In *Progress in Inorganic Chemistry*; Lippard, S. J., Ed.; John Wiley and Sons: New York, 1983; Vol. 30, p 1.
(34) Koopmans, T. *Physica* **1934**, *1*, 104.
(35) Gleiter, R.; Hyla-Kryspin, I.; Binger, P.; Regitz, M. *Organometallics* **1992**, *11*, 177.
(36) Veillard, A.; Demuynck, J. In *Modem Theoretical Chemistry*; Schaefer, H. F., Ed.; Plenum Press: New York, 1977; Vol. 4, p 187.
(37) Boehm, M. C.; Gleiter, R.; Delgado-Pena, F.; Cowan, D. O. *J. Chem. Phys.* **1983**, *79*, 1154.
(38) Gleiter, R.; Hyla-Kryspin, I.; Herberich, G. E. *J. Organomet. Chem.* **1994**, *478*, 95.
(39) Hyla-Krispin, I.; Gleiter, R.; Herberich, G. E.; Benard, M. *Organometallics* **1994**, *13*, 1795.

Table 5. Vertical Ionizations Energies, $I_{v,j}$ (eV), of the PE Spectra of **1**, **6**, **8**, and **9**

$I_{v,j}$(**8**)	$I_{v,j}$(**9**)	$I_{v,j}$(**6**)	assignt[a]	$I_{v,j}$(**1**)	assignt[a]
7.33	6.74	6.70	Co t_{2g} (la′, 1a″, 2a″)	6.6	Co t_{2g} (la′−3a′, la″−3a″)
7.70	7.14	7.10		6.9	Cb π (7a″, 6a″)
8.10	7.39	7.30	Cb π (4a″, 3a′)	7.5	Cb π (7a′, 6a′)
9.93	8.84	8.70	Cp π (3a″, 2a′)	8.6	Cp π (4a′, 4a″, 5a′, 5a″)

[a] The MO labeling refers to Table 4.

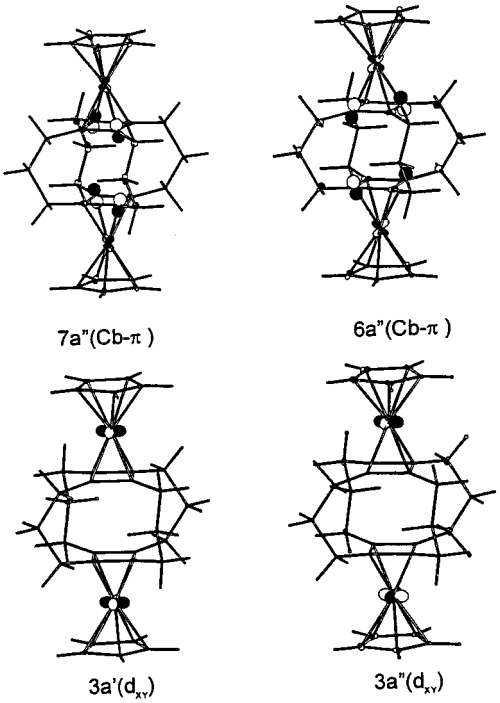

Figure 9. Highest occupied ligand and metal orbitals of **1**.

Since **1** and **2** are symmetrical molecules, it is clear that the molecular orbital wave functions will be delocalized on symmetry-equivalent sites. Thus, in the valence region of **1** and **2** we find in-phase and out-of-phase symmetry-adapted combinations of the MOs of two mononuclear units such as **8**. As an example we show in Figure 9 the HOMO (7a″), HOMO − 1(6a″), and two cobalt levels (3a′, 3a″) of **1**. The calculated Koopmans ionization energies corresponding to eight ligand π and six Co t_{2g} combinations are collected in Table 4.

The inductive effect of the CH_2 chains on the Cb ligands shifts the ionizations originating in Cb π MOs and Co t_{2g} levels of **1** and **2** to lower energies with respect to that of **8**. Due to the close proximity of both CpCoCb units in **1**, the out-of phase linear combinations (7a″, 6a″) are separated from the in-phase ones (7a′, 6a′) by 1 eV. In **2** the corresponding π MOs are almost degenerate due to the large separation between the CpCoCb units. The Cp π MO s of **1** and **2** are almost degenerate and as in the case of **8** well separated from Cb π levels (1.85 eV (**1**), 3.17 eV (**2**)). The integrated natural charges of the ligands and cobalt atoms as well as the calculated occupation numbers for cobalt valence AOs are summarized in Tables 6 and 7.

II. HeI Photoelectron Spectrum of 1. The HeI PE spectrum of **1** is displayed in Figure 10. Above 9.5 eV strongly overlapping bands are observed, characteristic of ionizations from the σ framework and the total symmetric π MOs of the ligands. At lower energy there are three distinct band systems with maxima at 6.6−6.9, 7.5, and 8.6 eV. The areas defined by the band envelopes in the approximate ratio 8:2:4 provide an estimate of the number of ionizations associated with each band system.

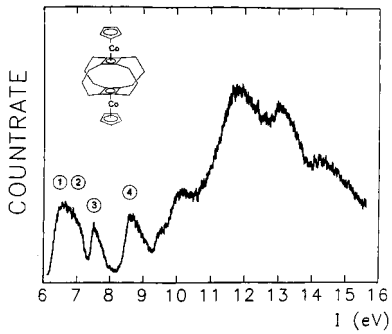

Figure 10. HeI photoelectron spectrum of **1**.

Assignments of bands in the PE spectrum of **1** are aided by earlier results[39] on the PE spectra of **8**, $(C_4Me_4)Co(C_5H_5)$ (**9**), and **6**. On the basis of INDO calculations with Green's function formalism accounting for relaxation and correlation effects carried out on **8**, large Koopmans defects were obtained for the Co t_{2g} MOs, but only small ones were encountered for ionizations from the Cb π and Cp π MOs. These calculations predicted in the case of **8** three doublet states arising from ionizations originating in Co t_{2g} levels on top of two ionic states from the HOMOs (Cb π) and two states from the Cp ligands. The vertical ionization energies of the PE spectra of **1**, **6**, **8**, and **9** are compared in Table 5.

On the basis of the comparisons in Table 5, and in concert with earlier results on dinuclear cobalt complexes,[40] we assign the first broad band in the PE spectrum of **1** (6.6−6.9 eV) to overlapping ionizations originating from six Co 3d (la′−3a′, la″−3a″) and two Cb π (7a″, 6a″) levels. Taking into account that for delocalized ligand MOs Koopmans defects are less important, the next two peaks at 7.5 and 8.6 eV correlate with ionization from Cb π (7a′, 6a′) and Cp π (4a′, 4a″, 5a′, 5a″) MOs. These assignments are in accord with the calculated splitting between the out-of-phase (7a″, 6a″) and the in-phase (7a′, 6a′) Cb π combinations as well as with the calculated separation of the MOs from the almost 4-fold degenerate Cp π (4a′, 4a″, 5a′, 5a″) levels (Table 4). Our tentative assignment suggests negative Koopmans defects of −0.34 and −0.21 eV for ionizations from Cb 7a″ and 6a″ MOs and 0.28−1.03 eV for ionizations from the remaining ligands levels. For ionizations from Co t_{2g} MOs Koopmans defects of 5.4−8.8 eV are predicted (Tables 4 and 5). These values agree very well with those calculated at the ab initio CI level for sandwich and triple-decker CO (d^6) compounds, and are consistent with the expected influence of relaxation and correlation on ionization energies originating in Co 3d levels. The appearance of metal ionizations on top of ligand ionizations seems to be a common feature of

(40) (a) Doran, M.; Hillier, I. H.; Seddon, E. A.; Seddon, K. R.; Thomas, V. H.; Guest, M. F. *Chem. Phys. Lett.* **1979**, *63*, 612. (b) Van Dam, H.; Oskam, A. In *Transition Metal Chemistry*; Melson, G. A., Figgis, B. N., Eds.; Marcel Dekker, Inc.: New York, 1985; Vol 9, p 125. (c) Cauletti, C.; Green, J. C.; Kelly, M. R.; Powell, P.; van Tilborg, J.; Robbins, J.; Smart, J. *J. Electron Spectrosc. Relat. Phenom.* **1980**, *19*, 327. (d) Hiller, I. H. *Pure Appl. Chem.* **1979**, *51*, 2183. (e) Boehm, M. C.; Gleiter, R. *J. Comput. Chem.* **1982**, *3*, 140. (f) Boehm, M. C.; Gleiter, R.; Herberich, G. E.; Hessner, B. *J. Phys. Chem.* **1985**, *89*, 2129. (g) Boehm, M. C.; Gleiter, R. *Chem. Phys. Lett.* **1986**, *123*, 87; *Theor. Chim. Acta* **1980**, *57*, 315.

Table 6. Occupation Numbers of Co Valence AOs, Natural Charge, and ΔSCF (eV) Values for Broken Symmetry Doublet States of $\mathbf{1}^+$ and $\mathbf{2}^+$

	$^2\mathbf{1}^+$ (Co1 d_{xy})		$^2\mathbf{1}^+$(HOMO)		$^2\mathbf{2}^+$(Co1 d_{xy})		$^2\mathbf{2}^+$(HOMO)	
NAO	Co1	Co2	Co1	Co2	Co1	Co2	Co1	Co2
$3d_{xy}$	1.106	1.976	1.979	1.979	1.004	1.977	1.978	1.978
$3d_{x^2-y^2}$	1.898	1.965	1.965	1.965	1.963	1.967	1.976	1.976
$3d_{z^2}$	1.996	1.995	1.996	1.996	1.995	1.995	1.996	1.996
$3d_{xz}$	1.498	1.049	1.208	1.212	1.269	1.067	1.133	1.011
$3d_{yz}$	1.427	1.038	0.861	0.859	1.269	1.062	0.957	1.082
4s	0.139	0.122	0.126	0.125	0.142	0.125	0.116	0.116
			Charge					
q(Co1)	+0.875		+0.800		+1.296		+0.785	
q(Co2)	+0.783		+0.795		+0.749		+0.781	
q(Cbl)	+0.244		−0.049		+0.119		−0.055	
q(Cb2)	−0.360		−0.093		−0.351		−0.046	
q(Cp1)	−0.266		−0.234		−0.515		−0.232	
q(Cp2)	−0.276		−0.237		−0.298		−0.233	
ΔSCF	4.68		5.25		2.58		6.26	

the PE spectra of electron-rich first-row transition-metal compounds.[35−41]

III. Ground-State Electronic Structures of $\mathbf{1}^+$ and $\mathbf{2}^+$. For $\mathbf{1}^+$ and $\mathbf{2}^+$ we performed open-shell calculations within the UHF framework with and without symmetry restrictions on the wave functions. Since the results obtained with symmetrical wave functions do not agree with the PE results, we will only discuss those obtained for symmetry-broken solutions (Table 6).

These calculations predict only small differences for the ionization process from the ligand. The wave functions of the cationic states $^2\mathbf{1}^+$(HOMO) and $^2\mathbf{2}^+$(HOMO) differ little from those of the symmetry-adapted states $^2A''$ ($\mathbf{1}^+$) and ^2A_g ($\mathbf{2}^+$). Substantial differences are observed, however, for cobalt ionizations. The computational results are symmetry-broken localized hole states with lower total energies than in the case of symmetry-adapted states. We notice that there are many cases known in the literature, especially for deep core electron ionizations, where the SCF solution lowest in energy exhibits a lower symmetry than the full Hamiltonian.[42] The calculated relaxation energy for the doublet state $^2\mathbf{1}^+$(Co1 d_{xy}) is about 2 times greater than in the symmetric $^2A'$ state (eq 1).[43] As a

$$E_{\text{relax}}(\text{loc}) \approx 2E_{\text{relax}}(\text{deloc}) \qquad (1)$$

consequence of eq 1 the first ionization in the PE spectrum of **1** is cobalt-based and is reasonably separated from the ionization process of the Cb π HOMO. The same relation was found by Böhm et al. for the cationic hole states of a bis(fulvalene)diiron complex examined with Green's function formalism within the INDO framework.[37] As already mentioned, upon ionization of metal 3d electrons, the electron density flows from the surrounding ligands toward the metal to ensure a near constancy of the metal net charge in the ground state of the neutral molecule and in the ionized state. Although the ionizations of **1** and **2** *both* involve a single metal site, this reorganization of electron density is not quantitatively equal for $\mathbf{1}^+$ and $\mathbf{2}^+$ (Table 7).

Table 7. Charge Reorganizations Δ*q* in the Cobalt-Localized Hole States of $\mathbf{1}^+$ and $\mathbf{2}^+$ Calculated with Respect to Neutral Molecules

Δ*q*[a]	$^2\mathbf{1}^+$(Co1 d_{xy})	$^2\mathbf{2}^+$(Co1 d_{xy})	Δ*q*[a]	$^2\mathbf{1}^+$(Co1 d_{xy})	$^2\mathbf{2}^+$(Co1 d_{xy})
Co1	−0.155	−0.572	Co2	−0.062	−0.025
Cb1	−0.586	−0.490	Cb2	+0.018	−0.020
Cp1	−0.112	+0.164	Cp2	−0.102	−0.053

[a] Negative/positive signs mean loss/gain of electron density upon ionization.

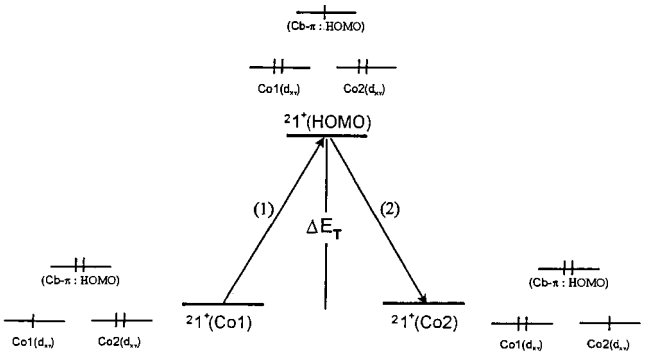

Figure 11. Proposed IT mechanism in $\mathbf{1}^+$ involving hole state transfer from Co_1 to Co_2 through the cyclobutadiene π MO.

Discussion

The positive charge in the pentano-bridged monocation is almost perfectly localized on one cobalt atom, with the relative charges on the two metals calculated as 96:4 for $\mathbf{2}^+$. In $\mathbf{1}^+$, however, the cobalt charge densities are calculated to have the ratio 71:29. This means that, upon ionization of an electron from cobalt and after relaxation in $\mathbf{1}^+$, the loss of metal electron density amounts to 71% for Co1 and 29% for Co2. In contrast, $\mathbf{2}^+$ may be regarded as a valence-trapped species *without* significant interactions between the molecular halves. Due to relaxation associated with ionization of an electron from cobalt in one molecular half, and in spite of recompensations from neighboring ligands, 0.098e ($\mathbf{2}^+$) and 0.146e ($\mathbf{1}^+$) are recompensated by the second half.

In Figure 11 we present a two-step mechanism for electron transfer from one cobalt atom to the other. One starts at the left side of Figure 11 with the ground state of the cation $\mathbf{1}^+$, a hole state mainly localized at the $3d_{xy}$ orbital of Col. In the first step the hole is filled from an electron of the Cb π orbital, the HOMO of **1**. In the second step the hole in the Cb π MO relaxes to the ground state in which it is localized at the $3d_{xy}$ orbital of Co2. This mechanism is known in the literature as "hole transfer" [15,44] because the concerted result is that of a positive hole moving from left to right, i.e., from one cobalt atom to the other one, via the Cb π HOMO. The transannular electron transfer most likely involves a through-bond mechanism, since σ CH_2 character is demonstrable in the Cb π orbital (Figure 9).

Quantitatively, a smaller gap, Δ*E*, between the total energies of the corresponding doublet states is expected to lead to a greater degree of metal−metal coupling. The calculated Δ*E* values are 0.57 eV for $\mathbf{1}^+$ and 3.65 eV for $\mathbf{2}^+$. These results are in agreement with the differences in calculated charges on the two Co centers in $\mathbf{1}^+$ and $\mathbf{2}^+$ and with the relative IR shifts in $\mathbf{4}^+$ and $\mathbf{5}^+$. Furthermore, the ligand-to-metal charge-transfer band in the near-IR region predicted for $\mathbf{1}^+$ ($\Delta E = 0.57$ eV, 4600 cm^{-1}) is indeed observed at $\Delta E = 0.71$ eV (6100 cm^{-1}).

(41) (a) Stahl, L.; Ma, H.; Ernst, R. D.; Hyla-Kryspin, I.; Gleiter, R.; Ziegler, M. L. *J. Organomet. Chem.* **1987**, *326*, 257. (b) Gleiter, R.; Hyla-Kryspin, I.; Ziegler, M. L.; Sergeson, G.; Green, J. C.; Stahl, L.; Ernst, R. D. *Organometallics* **1989**, *8*, 298.

(42) (a) Cederbaum, L. S.; Domcke, W. *J. Chem. Phys.* **1977**, *66*, 5084. (b) Bagus, P. S.; Schaefer, H. F. *J. Chem. Phys.* **1972**, *56*, 224. (c) Lozes, R. L.; Goscinski, O.; Wahlgren, U. I. *Chem. Phys. Lett.* **1979**, *63*, 77. (d) Agren, H.; Bagus, P. S.; Roos, B. O. *Chem. Phys. Lett.* **1981**, *82*, 505. (e) Benard, M. *Chem. Phys. Lett.* **1983**, *96*, 183. (f) Schwarz, W. H. E.; Chang, T. C.; Seeger, U.; Hwang, K. H. *Chem. Phys.* **1987**, *117*, 73.

(43) For our case $E_{\text{relax}}(\text{loc}) = -\epsilon_i(\text{Koopmans}) - \Delta(\text{SCF(loc)}) = 12.76 - 4.68 = 8.08$ eV and $E_{\text{relax}}(\text{deloc}) = -\epsilon_i(\text{Koopmans}) - \Delta(\text{SCF(deloc)}) = 12.76 - 8.60 = 4.16$ eV.

(44) Hupp, J. T. *J. Am. Chem. Soc.* **1990**, *112*, 1563.

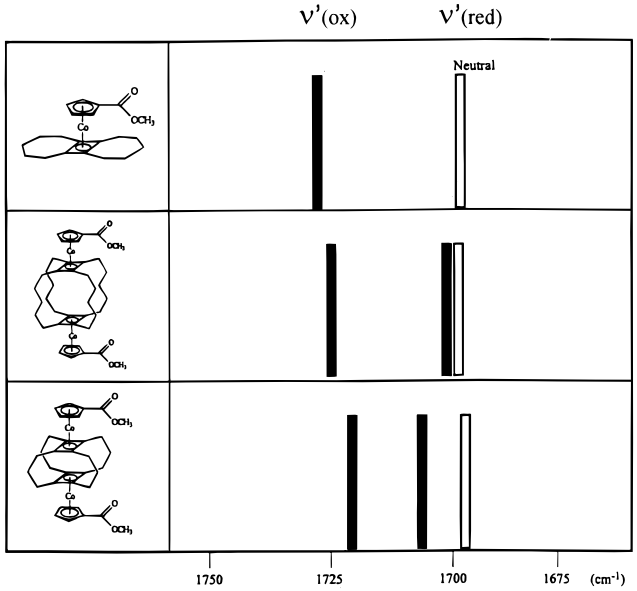

Figure 12. A line representation of the carbonyl absorption energies of the Co(I) complexes and their oxidation products. The labeled energies are defined in the text. The open bar gives the energy for the neutral Co(l) complexes; the solid bars give the energies of the two bands observed for the mixed-valent monocations $\mathbf{5}^+$ (middle) and $\mathbf{4}^+$ (bottom).

The weak interaction between metal centers in the pentano-bridged complex $\mathbf{2}^+$ is reminiscent of some results from earlier literature[45−47] which revealed that weak-to-moderate interactions are possible between metal centers in mixed-valent states of dinuclear *cyclophane* complexes. In contrast, a significantly greater degree of interaction between the metal centers in the propano-bridged *superphane* dinuclear ion $\mathbf{1}^+$ is implied by the rather large separation of the oxidation potentials of **1** ($\Delta E_{1/2}$ of almost 400 mV) and by its possession of an intense narrow intervalence transition band, the energy of which displays a modest dependence on the solvent dielectric parameter. IR spectroscopy of $\mathbf{1}^+$ proves, however, that the ion is not intrinsically delocalized. Although it is possible that the ion is delocalized on time scales longer than that of a molecular vibration,[48] theoretical calculations provide an alternative explanation to that of time scale differentials. They show that although the *spin is localized* on half of the molecule in $\mathbf{1}^+$ (in the semioccupied MO, the SOMO), the *charge is more equally shared* (ca. 70:30) between the metal centers through inductive interactions involving orbitals other than the SOMO.

The quantitative IR shifts for $\mathbf{4}^+$ and $\mathbf{5}^+$ may also be used to estimate relative charges on the two metal centers of the odd-electron species. Let the values of ν_{CO} be ν'(red) and ν'(ox), respectively, for the *fully* reduced and oxidized forms of a redox pair that describes the electron-transfer sites in a dinuclear complex (Figure 12). If the measured energies in the *mixed-valent* species are ν_{meas}(ox) and ν_{meas}(red) for the oxidized and reduced sites, respectively, then we can define a "charge distribution parameter", $\Delta\rho$, given by eq 2. The values of ν'-

$$\Delta\rho = \{[\nu'(\text{ox}) - \nu_{meas}(\text{ox})] + [\nu_{meas}(\text{red}) - \nu'(\text{red})]\}/2[\nu'(\text{ox}) - \nu'(\text{red})] \quad (2)$$

(red) and ν'(ox) may be obtained from studies on mononuclear analogues (e.g., $\mathbf{7}/\mathbf{7}^+$ in the present case), or from the IR energies of the fully reduced and oxidized forms of the dinuclear system (**5** and $\mathbf{5}^{2+}$ in the present case). Either set of values gives equivalent conclusions for the complexes under study.

Defined as in eq 2, the charge distribution parameter has a value of zero if the IR energies of the oxidized and reduced sites in the mixed-valent ion have exactly the values expected for the full change in oxidation state, and the value 0.5 if the IR energies of the two sites are equal. $\Delta\rho$ is thus an approximation of the residual charge found on the "innocent" redox site of a trapped-valent system. The upper limit of 0.5 implies complete sharing of the charge between the two sites, i.e., a fully delocalized system.

In the evaluation of this parameter for $\mathbf{4}^+$ and $\mathbf{5}^+$, we use $\nu'(\text{ox}) = 1722\ \text{cm}^{-1}$ and $\nu'(\text{red}) = 1696\ \text{cm}^{-1}$ (Table 2), giving $\Delta\rho$ values for $\mathbf{4}^+$ and $\mathbf{5}^+$ of 0.21 and 0.02, respectively. The former suggests a charge distribution between the two metals of 79:21, in excellent agreement with the ratio 71:29 calculated by UHF methods. The near-zero value for $\mathbf{5}^+$ informs us that charge as well as spin is localized on half of the mixed-valent ion with pentano bridges.

Concluding Remarks

Within the highly active field[6] of mixed-valent chemistry, the present results are relevant to the broad questions of how structure and matrix[30] influence the transition between localized and delocalized behavior between strongly-interacting metal centers.[11−17,49−51] The time scales inherent to the physical probes of the mixed-valent states are, in some cases, crucially important.[12,13,49] A discussion by Demadis et al. is particularly informative. In explaining the behavior of Os(II)Os(III) systems, at least one of which has physical characteristics similar to those of $\mathbf{1}^+$ and $\mathbf{4}^+$ (localized by IR but delocalized characteristics for the IT band), they focus on the slower time scale of solvent dipole reorganizations compared to that of molecular vibrations.[12] Similar arguments can be made to explain the combination of IR and optical absorbances observed for our propano-bridged systems. Superphanes with short transannular bridges may be helpful in further defining the localized-to-delocalized transition owing in part to their structural rigidity, and studies are planned involving alterations of both the electron-transfer site and the nature of the bridges.

Acknowledgment. We gratefully acknowledge support of this work at the University of Vermont by the National Science Foundation (Grant NSF CHE97-05763) and at the University of Heidelberg by Deutsche Forschungsgemeinschaft (Grant SFB 247), the Fonds der Chemischen Industrie, and the BASF Aktiengesellschaft.

Supporting Information Available: Two figures, one showing a first derivative of the visible spectrum of $\mathbf{6}^+$, the other giving a plot of $1/D_{op} - 1/D_s$ for the IT band of $\mathbf{1}^+$ (PDF).

JA9914792

(45) Bowyer, W. J.; Geiger, W. E.; Boekelheide, V. *Organometallics* **1984**, *3*, 1079.
(46) Voegeli, R. H.; Kang, H. C.; Finke, R. G.; Boekelheide, V. *J. Am. Chem. Soc*. 1986, *108*, 7010.
(47) Plitzko, K.-D.; Boekelheide, V. *Organometallics* **1988**, *7*, 1573.
(48) ESR spectroscopy is one probe with which to interrogate the longer time scale behavior of the mixed-valent systems. Unfortunately, however, solutions of $\mathbf{1}^+$ or $\mathbf{2}^+$ are ESR-silent, owing almost surely to rapid relaxation effects. Frozen solution spectra were obtained at 4 K which showed a single Co hfs for $\mathbf{2}^+$, but spectra of $\mathbf{1}^+$ under these conditions still had linewidths so great that hyperfine splittings were not visible.
(49) Ito, T.; Hamaguchi, T.; Nagino, H.; Yamaguchi, T.; Washington, J.; Kubiak, C. P. *Science* **1997**, *277*, 660.
(50) Lu, H.; Petrov, V.; Hupp, J. T. *Chem. Phys. Lett.* **1995**, *235*, 521.
(51) Bruns, W.; Kaim, W.; Waldhor, E.; Kreycik, M. *Inorg. Chem.* **1995**, *34*, 663.